

Elastic fields in superconductors caused by moving vortices

V. G. Kogan\*

Ames Laboratory, Ames, Iowa 50011, USA



(Received 17 October 2019; published xxxxxx)

Strains in superconductors due to moving vortices and vortex lattices are discussed. It is shown that the energy stored in elastic strains increases with vortex velocity. For moving vortex lattices, the elastic energy depends on velocity orientation relative to the lattice having minimum for the velocity directed along one of the unit cell vectors of the moving lattice. It is shown that for supersonic motion, the vortex-induced stress field has a shape similar to supersonic shock waves.

DOI: 10.1103/PhysRevB.00.004500

I. INTRODUCTION

The subject of this work are vortex induced strains in superconductors, which are related to the stress dependence of the critical temperature  $\partial T_c / \partial p$ . It turned out that this derivative in pnictides, and in  $\text{Ca}(\text{Fe}_{1-x}\text{Co}_x)_2\text{As}_2$  in particular [1], by one or two orders of magnitude exceeds values for conventional superconductors, making Fe-based pnictides favorable for observation of magnetoelastic effects.

Still, experimental evidence for strains in the mixed state in the absence of pinning is scarce. In Ref. [2], the experimental disagreement with predicted by the London theory vortex lattice structure in  $\text{NbSe}_2$  in tilted fields was attributed to extra magnetoelastic interactions of vortices. Such comparisons are difficult because complete sets of elastic moduli are usually unavailable. Besides, vortex lattices are extremely sensitive to a multitude of factors such as electronic band structure, order parameter symmetry, etc.

The stress due to vortices should affect the free energy of the system proportional to their number, i.e., to the magnetic induction  $B$ , and—along with energy—the equilibrium magnetization  $M$  [3]. This was suggested as a reason for the hump in reversible  $M(B)$  observed in  $\text{La}_{1.45}\text{Nd}_{0.40}\text{Sr}_{0.15}\text{CuO}_4$ , and  $\text{CeCoIn}_5$  [4,5]. The data on reversible  $M(B)$  are extremely rare since they imply absence of pinning.

Hence, as it stands today, the existence of vortex-induced strains and the magnetoelastic intervortex interactions are still to be confirmed. It is hard to expect progress in microscopic description of vortex-induced strains at arbitrary temperatures, although near  $T_c$  progress has been made [6,7]. For this reason, the London approach within which the core is represented by a  $\delta$  function deserves a try, though clearly it sweeps under the rug many important questions. Nevertheless, given a long history of London approach in describing magnetic properties of type-II superconductors, one can hope that applying it to magnetoelastic effects might be useful.

Magnetoelastic interactions are long range and, their weakness notwithstanding, should affect the mixed state in general [2,3,6], intervortex interactions [8], and vortex lattice

structures in particular [9]. In this paper, the focus is on magnetoelastic effects caused by moving vortices.

The vortex core of a size  $\xi$ , the coherence length, is not the only source of elastic strains. Supercurrents around the core, which extend to distances  $\sim \lambda$  are argued to contribute even more to strains because usually  $\lambda \gg \xi$  [6,7]. Since the currents decay exponentially, the corresponding strain source can be considered as local, its relatively large size notwithstanding. Hence, at distances  $r \gg \lambda$  this source can be considered as pointlike, and the approach developed below for core-size sources can be generalized to  $\lambda$ -size sources by a proper rescaling.

II. ELASTIC ENERGY OF VORTEX AT REST

Nucleation of the normal vortex core strains the host superconductor, since the normal phase has a larger specific volume as compared to superconductor. The relative volume change  $\zeta$  is related to the pressure dependence of the condensation energy or of the critical field  $H_c$  [10]:

$$\zeta = \frac{V_n - V_s}{V_s} = \frac{H_c}{4\pi} \frac{\partial H_c}{\partial p}. \tag{1}$$

The elastic energy density in isotropic solids reads:

$$F = \lambda u_{ij}^2 / 2 + \mu u_{ij}^2. \tag{2}$$

Here,  $u_{ij}$  is the strain tensor and  $\lambda, \mu$  are Lamé coefficients; summation over double indices is implied [11]. The stress tensor  $\sigma_{ij} = \partial F / \partial u_{ij} = \lambda u_{ll} \delta_{ij} + 2\mu u_{ij}$ , and the equilibrium condition  $\partial \sigma_{ij} / \partial x_j = \sigma_{ij,j} = 0$  is

$$\lambda u_{ll,i} + 2\mu u_{ij,j} = 0. \tag{3}$$

For a single vortex along  $z$  at the origin, the displacement  $\mathbf{u} = (u_x, u_y, 0)$  is radial in the plane  $xy$ , i.e.,  $\text{curl } \mathbf{u} = 0$  or  $\mathbf{u} = \nabla \chi$ , and  $u_{\alpha\beta} = \chi_{,\alpha\beta}$  where  $\chi$  is a scalar and  $\alpha, \beta$  acquire only  $x$  and  $y$  values. The equilibrium condition (3) reads  $(\lambda + 2\mu)\chi_{,\alpha\beta\beta} = 0$  with the first integral

$$\chi_{,\beta\beta} \equiv \nabla^2 \chi = C = \text{const}. \tag{4}$$

To fix this constant, one notes that  $\chi_{,\beta\beta} = u_{\beta\beta}$  describes compression and is related to the hydrostatic pressure within the system. For the problem of the strain caused by a single

\*kogan@ameslab.gov

82 vortex in otherwise unrestrained crystal, the pressure is zero,  
83 and one has to solve  $\nabla^2 \chi = 0$  under the boundary condition  
84  $u \rightarrow 0$  at large distances. Hence, the problem is the same as  
85 that of a linear charge in electrostatics, where the potential  
86 satisfies

$$\nabla^2 \chi = A \delta(\mathbf{r}), \quad (5)$$

87 where  $A$  is related to the linear charge density. From a simple  
88 core model as a normal cylinder of a size  $\xi$  follows [2]:

$$A = 2\pi \xi^2 \gamma, \quad \gamma = \frac{\zeta(\lambda + \mu)}{2(\lambda + 2\mu)}. \quad (6)$$

89 One, then, has  $\chi = (A/2\pi) \ln r + \text{const.}$  and

$$\mathbf{u} = \frac{\gamma \xi^2 \mathbf{r}}{r^2}, \quad u_{\alpha\beta} = \frac{\gamma \xi^2}{r^2} \left( \delta_{\alpha\beta} - \frac{2}{r^2} x_\alpha x_\beta \right). \quad (7)$$

90 The elastic energy per unit length of a vortex is

$$\mathcal{E} = \int d^2 \mathbf{r} (\lambda u_{\alpha\alpha}^2 / 2 + \mu u_{\alpha\beta}^2). \quad (8)$$

91 According to Eq. (7)  $u_{\alpha\alpha} = 0$  and

$$u_{\alpha\beta}^2 = u_{xx}^2 + u_{yy}^2 + 2u_{xy}^2 = \frac{A^2}{2\pi^2 r^4}. \quad (9)$$

92 Integrating over  $r$  in Eq. (8) from  $\xi$  to  $\infty$ , one obtains:

$$\mathcal{E} = \frac{A^2 \mu}{2\pi \xi^2} = 2\pi \mu \xi^2 \gamma^2. \quad (10)$$

### 93 III. VORTEX MOVING WITH SUBSOND VELOCITY

94 If the vortex moves, the elastic displacement at a particular  
95 material point depends on time and the local equation of motion  
96 is  $\sigma_{\alpha\beta,\beta} = \rho \ddot{u}_\alpha$  where  $\ddot{\mathbf{u}} \equiv \partial^2 \mathbf{u} / \partial t^2$  and  $\rho$  is the material  
97 density.

98 For a point source of stress one has to add to the energy  
99 density a term  $\eta_{\alpha\beta} u_{\alpha\beta} \delta(\mathbf{r} - \mathbf{v}t)$ , so that the stress tensor  
100 has an addition  $\partial F / \partial u_{\alpha\beta} = \eta_{\alpha\beta} \delta(\mathbf{r})$ . In isotropic case  $\eta_{\alpha\beta} =$   
101  $\eta \delta_{\alpha\beta}$  and the equation of motion is  $(\lambda + 2\mu) \chi_{,\alpha\beta\beta} - \rho \ddot{\chi}_{,\alpha} =$   
102  $\eta \partial_\alpha \delta(\mathbf{r} - \mathbf{v}t)$ , with the first integral

$$(\lambda + 2\mu) \nabla^2 \chi - \rho \ddot{\chi} = \eta \delta(\mathbf{r} - \mathbf{v}t), \quad (11)$$

103 where the coefficient  $\eta$  is fixed by comparison with the static  
104 Eq. (5):  $\eta = A(\lambda + 2\mu)$ . Hence, we have

$$\nabla^2 \chi - \frac{1}{v_s^2} \ddot{\chi} = A \delta(\mathbf{r} - \mathbf{v}t), \quad (12)$$

105 where  $v_s = \sqrt{(\lambda + 2\mu)/\rho}$  is the longitudinal sound velocity  
106 [12].

107 Equation (12) is solved by Fourier transform

$$\chi(\mathbf{r}, t) = \int \frac{d^2 \mathbf{k} d\omega}{(2\pi)^3} \chi(\mathbf{k}, \omega) e^{i(\mathbf{k}\mathbf{r} - \omega t)}. \quad (13)$$

108 Transforming the right-hand side (RHS) of Eq. (12),

$$\begin{aligned} & \int_{-\infty}^{\infty} dt \int d\mathbf{r} \delta(\mathbf{r} - \mathbf{v}t) e^{-i(\mathbf{k}\mathbf{r} - \omega t)} \\ &= \int_{-\infty}^{\infty} dt e^{-i(\mathbf{k}\mathbf{v} - \omega)t} = 2\pi \delta(\mathbf{k}\mathbf{v} - \omega), \end{aligned} \quad (14)$$

one obtains:

$$\chi(\mathbf{k}, \omega) = 2\pi v_s^2 A \frac{\delta(\omega - \mathbf{k}\mathbf{v})}{\omega^2 - v_s^2 k^2}. \quad (15)$$

In real space

$$\chi(\mathbf{r}, t) = v_s^2 A \int \frac{d^2 \mathbf{k}}{4\pi^2} \frac{e^{i\mathbf{k}(\mathbf{r} - \mathbf{v}t)}}{(\mathbf{k}\mathbf{v})^2 - k^2 v_s^2}. \quad (16)$$

If  $v = 0$ , the static solution is recovered (the integral for  $v = 0$   
is divergent, but the derivative  $\partial_r \chi = A/2\pi r$  is the same as in  
the static case).

For the velocity  $\mathbf{v} = v\hat{x}$ , one has at  $t = 0$ :

$$\chi(\mathbf{r}, 0) = -\frac{A}{4\pi^2} \int \frac{d^2 \mathbf{k} e^{i\mathbf{k}r}}{(1 - V^2)k_x^2 + k_y^2}, \quad (17)$$

where the reduced velocity  $V = v/v_s < 1$ . This differs from  
the static solution by rescaling  $k_x \rightarrow \sqrt{1 - V^2} k_x$  or, in real  
space, by  $x \rightarrow x/\sqrt{1 - V^2}$ . In other words, for  $V < 1$ , the  
circles of constant  $\chi$  for the vortex at rest, become ellipses  
 $x^2/(1 - V^2) + y^2 = \text{const.}$  with the  $x$  semiaxis  $\sqrt{1 - V^2}$   
times shorter than that of  $y$ . Hence, the static potential  
 $\chi(x, y)$  is contracted in the direction of motion by the factor  
 $\sqrt{1 - v^2/v_s^2}$  and moves as a whole with the vortex velocity  $v$ .

The energy stored in the elastic distortion of a vortex  
moving with a constant velocity is time independent. To  
evaluate this energy one can use the potential (17) for  $t = 0$ .  
This evaluation can be done in real space. Since the static  
potential  $\chi = (A/4\pi) \ln(x^2 + y^2)$ , we have for the moving  
vortex

$$\chi = \frac{A}{4\pi} \ln \left( \frac{x^2}{1 - V^2} + y^2 \right) \quad (18)$$

(an irrelevant constant is omitted). Clearly, the lines of constant  
 $\chi$  (the circles for the vortex at rest) are elliptic with a  
short semiaxis  $\sqrt{1 - V^2}$  along the direction of motion; this  
ellipse is strongly squeezed when the velocity approaches that  
of the sound. The strains follow:

$$\begin{aligned} u_{xx} &= -\frac{A(x^2 - \beta^2 y^2)}{2\pi(x^2 + \beta^2 y^2)^2}, & u_{yy} &= \frac{A\beta^2(x^2 - \beta^2 y^2)}{2\pi(x^2 + \beta^2 y^2)^2}, \\ u_{xy} &= -\frac{A\beta^2 xy}{\pi(x^2 + \beta^2 y^2)^2}, & \beta^2 &= 1 - V^2. \end{aligned} \quad (19)$$

The elastic energy (8) can now be evaluated as shown in  
Appendix A:

$$\mathcal{E} = \frac{A^2(1 + \beta^2)}{16\pi \xi^2 \beta^3} \left[ \frac{\lambda}{2}(1 - \beta^2)^2 + \mu(1 + \beta^2)^2 \right]. \quad (20)$$

This gives for low velocities  $V = v/v_s \ll 1$ :

$$\mathcal{E} \approx \frac{A^2 \mu}{2\pi \xi^2} \left( 1 + \frac{\lambda + 3\mu}{8\mu} V^4 \right) \quad (21)$$

with correct limit (10) for  $V = 0$ . If the velocity approaches  
 $v_s$ , the elastic energy diverges as

$$\mathcal{E} \approx \frac{A^2}{16\sqrt{2}\pi \xi^2} \frac{\lambda + 2\mu}{(1 - V)^{3/2}}. \quad (22)$$

The elastic potential  $\chi(\mathbf{r}, t)$  obtained solving linear  
Eq. (12) is a partial solution of this equation with the source

141 term  $\propto \delta(\mathbf{r} - \mathbf{v}t)$  at the RHS. In fact, this equation has also  
 142 solutions of the homogeneous equation without the RHS,  
 143 i.e., of the wave equation  $\nabla^2 \chi - \ddot{\chi}/v_s^2 = 0$ . These are sound  
 144 waves generated by the moving elastic field; these waves carry  
 145 away energy and contribute to the vortex drag coefficient. This  
 146 problem, however, is out of the scope of this paper.

#### 147 IV. VORTEX LATTICE

##### 148 A. Static lattice

149 Consider now a two-dimensional periodic lattice of vor-  
 150 tices at positions  $\mathbf{a}$  in an infinite sample. As argued in Ref. [3],  
 151 the elastic potential in this case is a solution of

$$\nabla^2 \chi = A \left[ \sum_{\mathbf{a}} \delta(\mathbf{r} - \mathbf{a}) - \frac{B}{\phi_0} \right], \quad (23)$$

152 where  $B$  is the magnetic induction. In terms of electrostatic  
 153 analogy, the source term of the Poisson equation (23) must  
 154 have a negative background density  $B/\phi_0$  to make the system  
 155 quasineutral for the equation to have periodic finite solutions  
 156 on the whole plane.

157 One looks for  $\chi(\mathbf{r})$  as Fourier series

$$\chi(\mathbf{r}) = \sum_{\mathbf{G}} \chi(\mathbf{G}) e^{i\mathbf{G}\mathbf{r}}, \quad \chi(\mathbf{G}) = \frac{B}{\phi_0} \int d\mathbf{r} \chi(\mathbf{r}) e^{-i\mathbf{G}\mathbf{r}} \quad (24)$$

158 with  $\mathbf{G}$  being the reciprocal lattice vectors. Transforming the  
 159 RHS of Eq. (23) one can use identities [13]:

$$\sum_{\mathbf{a}} \delta(\mathbf{r} - \mathbf{a}) = \frac{B}{\phi_0} \sum_{\mathbf{G}} e^{i\mathbf{G}\mathbf{r}}, \quad \frac{B}{\phi_0} = \frac{B}{\phi_0} \sum_{\mathbf{G}} \delta_{\mathbf{G},0} e^{i\mathbf{G}\mathbf{r}}, \quad (25)$$

160 where the symbol  $\delta_{0,0} = 1$  and  $\delta_{\mathbf{G},0} = 0$  for  $\mathbf{G} \neq 0$ . One then  
 161 obtains:

$$\chi(\mathbf{G}) = -\frac{2\pi\gamma\xi^2 B}{\phi_0 G^2} (1 - \delta_{\mathbf{G},0}). \quad (26)$$

162 Being transformed to real space, the part of  $\chi(\mathbf{G})$  containing  
 163  $\delta_{\mathbf{G},0}$  generates an uncertain constant,

$$\sum_{\mathbf{G}} \frac{1 - \delta_{\mathbf{G},0}}{G^2} e^{i\mathbf{G}\mathbf{r}} = \sum_{\mathbf{G} \neq 0} \frac{e^{i\mathbf{G}\mathbf{r}}}{G^2} + \text{const.}, \quad (27)$$

164 which is coordinate independent and therefore irrelevant.

##### 165 B. Moving lattice

166 If the lattice moves, the vortex positions are  $\mathbf{a} + \mathbf{v}t$  where  
 167  $\mathbf{a}$  define the lattice at  $t = 0$ . The elastic potential obeys

$$\nabla^2 \chi - \frac{\ddot{\chi}}{v_s^2} = A \left[ \sum_{\mathbf{a}} \delta(\mathbf{r} - \mathbf{v}t - \mathbf{a}) - \frac{B}{\phi_0} \right]. \quad (28)$$

168 One now employs the Fourier transform

$$\chi(\mathbf{r}, t) = \sum_{\mathbf{G}} \int \frac{d\omega}{2\pi} \chi(\mathbf{G}, \omega) e^{i(\mathbf{G}\mathbf{r} - \omega t)}, \quad (29)$$

$$\chi(\mathbf{G}, \omega) = \frac{B}{\phi_0} \int d\mathbf{r} dt \chi(\mathbf{r}, t) e^{-i(\mathbf{G}\mathbf{r} - \omega t)}, \quad (30)$$

see Appendix B, to obtain:

$$\chi(\mathbf{G}, \omega) = \chi_0 \frac{\delta(\omega - \mathbf{G}\mathbf{v}) - \delta(\omega)\delta_{\mathbf{G},0}}{\omega^2 - G^2 v_s^2} \quad (31)$$

$$\chi_0 = \frac{4\pi^2 B \gamma \xi^2 v_s^2}{\phi_0} = \frac{2\pi B \gamma v_s^2}{H_{c2}}. \quad (32)$$

Hence, only the frequencies  $\omega = \mathbf{G}\mathbf{v}$  are present in the Fourier  
 170 transform over time [14]. One could expect this because an  
 171 observer of a moving vortex lattice should register the main  
 172 period  $a_1/v \propto 1/G_1 v$  where  $a_1$  is the real space lattice period  
 173 and  $G_1$  is the corresponding reciprocal vector.  
 174

##### 175 C. Elastic energy of moving lattice

The quasistatic elastic energy density of the vortex lattice is

$$F = \frac{B}{\phi_0} \int_{\text{cell}} d\mathbf{r} (\lambda u_{\alpha\alpha}^2/2 + \mu u_{\alpha\beta}^2), \quad (33)$$

177 where the integration is extended over the unit cell. Being  
 178 interested in a stationary state, one can calculate the energy  
 179 at  $t = 0$ . Fourier components of the potential  $\chi$  at  $t = 0$  are

$$\begin{aligned} \chi(\mathbf{G}, 0) &= \int_{-\infty}^{\infty} \frac{d\omega}{2\pi} \chi(\mathbf{G}, \omega) \\ &= \frac{\chi_0}{2\pi} \left[ \frac{1}{(\mathbf{G}\mathbf{v})^2 - G^2 v_s^2} + \frac{\delta_{\mathbf{G},0}}{G^2 v_s^2} \right]. \end{aligned} \quad (34)$$

180 As in the static case, the last term here generates in real space  
 181 a coordinate independent constant, which can be disregarded  
 182 because only gradients of  $\chi$  have physical meaning.

183 After straightforward algebra one obtains:

$$F = \frac{\chi_0^2 (\lambda + 2\mu)}{2} \sum_{\mathbf{G} \neq 0} \frac{G^4}{[(\mathbf{G}\mathbf{v})^2 - G^2 v_s^2]^2}. \quad (35)$$

184 The sum here is divergent due to long-range elastic perturba-  
 185 tions. It can be evaluated numerically because, when treating  
 186 vortex cores as  $\delta$  functions, the maximum  $G$  should be of the  
 187 order of  $1/\xi$ .

188 One can now compare energies of hexagonal vortex lattices  
 189 moving with velocities  $\mathbf{v}$  oriented differently relative to the  
 190 lattice. Let the hexagonal lattice have one of the unit cell  
 191 vectors along the  $x$  axis:

$$\mathbf{a}_1 = a_0 \hat{x}, \quad \mathbf{a}_2 = a_0 (\hat{x} + \sqrt{3}\hat{y})/2, \quad a_0^2 = 2\phi_0/B\sqrt{3}, \quad (36)$$

that correspond to the reciprocal lattice

$$G_x = G_0 \frac{\sqrt{3}}{2} n, \quad G_y = G_0 \left( m - \frac{n}{2} \right), \quad G_0^2 = \frac{2B}{\phi_0 \sqrt{3}} \quad (37)$$

193 with integers  $n$  and  $m$ . The squared length of a lattice vector is  
 194  $G^2 = G_0^2 (n^2 - nm + m^2)$ . The velocity orientation is fixed by  
 195 the angle  $\alpha$  with the  $x$  axis:  $\mathbf{v} = v(\hat{x} \cos \alpha + \hat{y} \sin \alpha)$ . Hence,  
 196 we have for the sum in Eq. (35):

$$\begin{aligned} S(\mathbf{v}) &= v_s^4 \sum_{\mathbf{G} \neq 0} \frac{G^4}{[(\mathbf{G}\mathbf{v})^2 - G^2 v_s^2]^2} \\ &= \sum_{n^2 + m^2 \neq 0} \frac{(n^2 - nm + m^2)^2}{d(\alpha, n, m)}, \end{aligned}$$

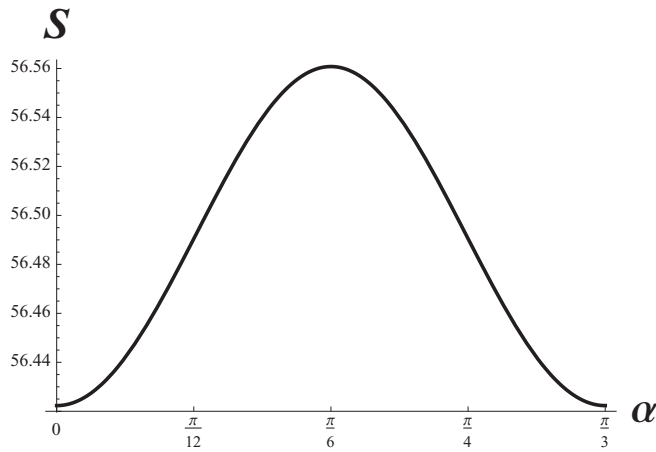


FIG. 1.  $S(\alpha)$  of Eq. (38) calculated for  $h = 0.1$  and  $V = v/v_s = 0.6$ .

$$d = [V^2(\sqrt{3}n \cos \alpha + (2m - n) \sin \alpha)^2/4 - (n^2 - nm + m^2)]^2, \quad (38)$$

where  $V = v/v_s$ . To ensure that the sum is not extended to  $G \gtrsim 1/\xi$ , we introduce in the numerator of the sum (38) a factor

$$\exp(-G^2\xi^2) = \exp[-h(n^2 - nm + m^2)],$$

$$h = \frac{2B\xi^2}{\phi_0\sqrt{3}} \sim \frac{B}{H_{c2}}. \quad (39)$$

Figure 1 shows the numerically evaluated  $S(\alpha)$  according to Eqs. (38) and (39) for  $v = 0.6 v_s$  and  $h = 0.1$  (or  $B/H_{c2} \approx 0.5$ ). It is seen that minimum energy corresponds to velocity directed along the unit cell vectors, i.e., to  $\alpha = 0$  and  $\alpha = \pi/3$ , whereas  $\alpha = \pi/6$  corresponds to the maximum energy. Although the difference  $S(\pi/6) - S(0)$  is of the order  $10^{-3}$ , it is worth recalling that in the isotropic case the hexagonal vortex lattice at rest is degenerate relative to arbitrary rotations. The difference  $\Delta S = S(\pi/6) - S(0)$  increases fast with increasing velocity.

The difference in elastic energies for the two orientations is

$$\Delta F \approx \frac{\chi_0^2 \tilde{\lambda}}{v_s^4} \Delta S \approx \left( \frac{B}{H_{c2}} \gamma \right)^2 \tilde{\lambda} \Delta S, \quad (40)$$

where  $\tilde{\lambda} \sim 10^{12}$  egr/cm<sup>3</sup> is an estimate for the elastic constants. Taking  $\gamma \sim \zeta \sim 10^{-5}$ , one obtains  $\Delta F \sim 10^{-3}$  erg/cm<sup>3</sup> for our example.

## V. SUPERSOUND VELOCITIES

Velocities of vortices up to  $\approx 1.5 \times 10^6$  cm/s have been recently recorded in Pb films [15], which is well above the sound speed in Pb of about  $2 \times 10^5$  cm/s. Vortices were crossing the narrow part of a thin-film bridge and were visualized with the help of sub- $\mu$ m-size scanning SQUID. The voltage and the current along the bridge were monitored that made it possible to evaluate vortex velocities. Vortices enter the bridge as a well formed and stable chain but slow down penetrating the bridge (the driving current decreases toward the strip middle) and at some points the chain splits in two or more parallel chains.

One may speculate that the elastic perturbations caused by fast-moving vortices play a role in forming vortex chains.

If a vortex moves with a supersonic velocity  $V > 1$ , Eq. (17) for the elastic potential at  $t = 0$  becomes

$$-\frac{4\pi^2 \chi(\mathbf{r}, 0)}{A} = \int \frac{d^2 \mathbf{k} e^{i\mathbf{k}\mathbf{r}}}{k_y^2 - \eta^2 k_x^2}, \quad \eta^2 = V^2 - 1 > 0. \quad (41)$$

The integration over  $k_y$  is done in the complex plane of  $k_y$ . The contour of integration for  $y > 0$  is chosen as a half-circle of a large radius in the upper half-plane, the real axis of  $k_y$ , and infinitesimal half-circles round the poles at  $k_y = \pm \eta k_x$  chosen as to leave the poles within the contour:

$$\int_{-\infty}^{\infty} \frac{dk_y e^{ik_y y}}{k_y^2 - \eta^2 k_x^2} = -\frac{y}{|y|} \frac{\pi \sin(k_x \eta y)}{\eta k_x}. \quad (42)$$

Integration over  $k_x$  then gives:

$$\chi(\mathbf{r}, \eta)_{t=0} = \frac{A}{4\eta} \theta(x + \eta|y|), \quad (43)$$

the  $\theta$  function here is unity for a positive argument and zero otherwise. The potential  $\chi(x, y)$  should be determined for  $x < 0$ , because no elastic perturbation can exist in front of a vortex moving with supersonic velocity. In fact, the potential  $\chi(x, y) = A/4\eta$  or zero, depending on what domain of  $x, y$  is chosen. These domains are separated by straight lines  $x + \eta y = 0$  and  $x - \eta y = 0$ , as shown in Fig. 2. The angle between two boundaries is

$$\alpha = 2 \cot^{-1} \eta. \quad (44)$$

In experiment of Ref. [15]  $v/v_s \approx 15/2 = 7.5$  that corresponds to the opening angle of the supersonic tail behind the vortex  $\alpha \approx 0.27 \approx 15^\circ$ .

When  $v \rightarrow v_s$  and  $\eta \rightarrow 0$ ,  $\alpha \rightarrow \pi$ , i.e., boundaries of the central domain open to coincide with the  $y$  axis. At large velocities  $\eta \gg 1$  and  $\alpha \approx 2/\eta \ll 1$ . This two-dimensional picture is reminiscent of shock wave fronts created by a supersonic motion of a body in continuous medium.

Within London model, the potential  $\chi$  changes discontinuously at these boundaries, i.e., the displacement  $\mathbf{u}$  has a

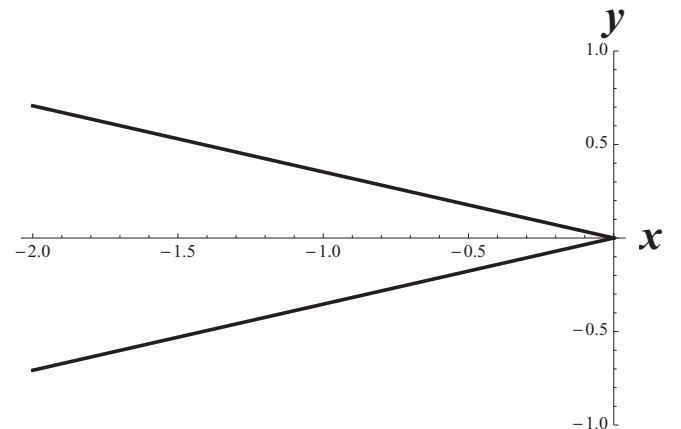


FIG. 2. Boundaries at which the potential  $\chi$  changes discontinuously for  $V = v/v_s = 3$ .  $\chi = 0$  between these boundaries and  $\chi = A/4\eta$  otherwise.

$\delta$ -function singularity at the boundaries. These discontinuities are the model artifacts since the vortex is considered as a point source of the elastic perturbation and is represented by  $\delta$  function. Clearly, in a better theory the discontinuity should be smeared over a belt of a width  $\sim \xi$  (or  $\lambda$ ), and the displacement will have a sharp maximum at the boundary and go to zero out of the belt. In turn, the strains related to second derivatives of  $\chi$  will have a sharp maximum on one side of the boundary and a sharp minimum on the other. Hence, as a consequence of a sharp displacement at the boundary, one expects the pressure enhancement on one side and the depression on the other. Interaction of other vortices with these pressure profiles is an open question.

## VI. SUMMARY AND DISCUSSION

It is shown that the rotational degeneracy of the hexagonal vortex lattice is removed by lattice motion due to vortex-induced strains. Moreover, the orientation of the moving lattice with one of the unit cell vectors along the velocity corresponds to minimum elastic energy. It is worth noting here that the same orientational effect has been predicted by considering pinning [16], the time-dependent Ginzburg-Landau or London models of moving vortex lattices [17,18].

In addition to reorientation of the moving lattice, elastic contribution to the intervortex interaction should cause distortions of the moving lattice structure as compared to the lattice at rest. Distortions of static lattices in tetragonal crystals were discussed in Refs. [3,9]. The stationary structure of a uniformly moving lattice can be found employing the minimum dissipation principle [18], the problem that would take us out of the main subject of this paper.

Experimentally, there are situations when the vortex velocities are very high. In flux avalanches in thin YBCO films, vortices are claimed to move with velocities up to  $5 \times 10^6$  cm/s [19]. In Pb films recently recorded vortex velocities reach  $10^6$  cm/s [15]. Hence, vortex velocities may approach and exceed  $v_s$ , the speed of sound. Within the model of this paper, however, the elastic energy diverges when  $v \rightarrow v_s$ . Clearly, the model should break down in this limit, because the energy of the vortex system cannot exceed the superconducting condensation energy. In other words, the superconducting phase should be strongly perturbed in this case, that would lead to velocity dependence of basic material parameters such as  $\zeta$ ,  $\xi$ ,  $A$ , considered as constants in this paper.

As mentioned, the elastic potential  $\chi(\mathbf{r})$  obtained solving Eq. (12) is only a partial solution corresponding to  $\delta(\mathbf{r} - \mathbf{v}t)$  at the RHS. In fact, this equation has also solutions for zero RHS, i.e., of the wave equation  $\nabla^2 \chi - \ddot{\chi}/v_s^2 = 0$ . These are sound waves that contribute to energy dissipation, i.e., to vortex drag coefficient. Of a special interest the sound generation is for a supersonic velocities, the subject of future work.

The density difference between the normal core and the superconducting surrounding is not the only reason for vortex-induced elastic perturbations discussed above. The nonuniform distribution of supercurrents around the vortex may also cause elastic distortions in the underlying crystal. The source of these distortions is localized in a region of a size  $\lambda$ , the

London penetration depth which is usually large relative to the core size  $\xi$  [6,7]. Elastic perturbations, though, decay only as a power law at  $r > \lambda$ , i.e., they are long range, hence their localized source can again be formally described by a  $\delta$  function. Hence, in principle, the formal treatment presented above can be applied in this case, too. The factor  $A$  of the  $\delta$  function will, of course, differ from that given in Eq. (5).

## ACKNOWLEDGMENTS

I thank A. Gurevich, E. Zeldov, R. Mints, and L. Boulaevskii for discussions and critical comments. This work was supported by the U.S. Department of Energy (DOE), Office of Science, Basic Energy Sciences, Materials Science and Engineering Division. The work was done at the Ames Laboratory, which is operated for the U.S. DOE by Iowa State University under Contract No. DE-AC02-07CH11358.

## APPENDIX A

To evaluate the energy (8) one needs:

$$(u_{\alpha\alpha})^2 = \frac{A^2(\beta^2 - 1)^2(x^2 - \beta^2 y^2)^2}{4\pi^2(x^2 + \beta^2 y^2)^4}, \quad (\text{A1})$$

$$\begin{aligned} u_{\alpha\gamma}^2 &= u_{xx}^2 + u_{yy}^2 + 2u_{xy}^2 \\ &= \frac{A^2(1 + \beta^4)(x^4 + \beta^4 y^4) - 2x^2 y^2 \beta^2(1 - 4\beta^2 + \beta^4)}{4\pi^2(x^2 + \beta^2 y^2)^4}. \end{aligned} \quad (\text{A2})$$

Further, one has:

$$\begin{aligned} I_1 &= \int d\mathbf{r} u_{\alpha\alpha}^2 \\ &= \frac{A^2(1 - \beta^2)^2}{4\pi^2} \int_{\xi}^{\infty} \frac{dr}{r^3} \int_0^{2\pi} d\varphi \frac{(\beta^2 \sin^2 \varphi - \cos^2 \varphi)^2}{(\cos^2 \varphi + \beta^2 \sin^2 \varphi)^4} \\ &= \frac{A^2(1 - \beta^2)^2(1 + \beta^2)}{16\pi \xi^2 \beta^3}. \end{aligned} \quad (\text{A3})$$

Further, one obtains:

$$I_2 = \int d\mathbf{r} u_{\alpha\gamma}^2 = \frac{A^2(1 + \beta^2)^3}{16\pi \xi^2 \beta^3}. \quad (\text{A4})$$

The sum  $\lambda I_1/2 + \mu I_2$  gives Eq. (20) of the main text.

## APPENDIX B

Apply  $\sum_{\mathbf{G}} \int d\omega/2\pi$  to the RHS of Eq. (28):

$$\begin{aligned} \sum_{\mathbf{a}} \delta(\mathbf{r} - \mathbf{v}t - \mathbf{a}) &= \frac{B}{\phi_0} \sum_{\mathbf{G}} e^{i\mathbf{G}(\mathbf{r} - \mathbf{v}t)} \\ &= \frac{2\pi B}{\phi_0} \sum_{\mathbf{G}} e^{i\mathbf{G}(\mathbf{r})} \int_{-\infty}^{\infty} d\omega e^{-i\omega t} \delta(\omega - \mathbf{G}\mathbf{v}). \end{aligned} \quad (\text{B1})$$

333 Hence, one has:

$$\sum_{\mathbf{a}} \delta(\mathbf{r} - \mathbf{v}t - \mathbf{a}) = \frac{2\pi B}{\phi_0} \sum_{\mathbf{G}} \int_{-\infty}^{\infty} \frac{d\omega}{2\pi} \delta(\omega - \mathbf{G}\mathbf{v}) e^{i(\mathbf{G}\mathbf{r} - \omega t)}. \quad (\text{B2})$$

Further, one uses

$$\frac{B}{\phi_0} = \frac{2\pi B}{\phi_0} \sum_{\mathbf{G}} \int_{-\infty}^{\infty} \frac{d\omega}{2\pi} \delta_{\mathbf{G},0} \delta(\omega) e^{i(\mathbf{G}\mathbf{r} - \omega t)}. \quad (\text{B3})$$

to obtain Eqs. (31) and (32).

334

335

- 
- [1] E. Gati, S. Köhler, D. Guterding, B. Wolf, S. Knöner, S. Ran, S. L. Bud'ko, P. C. Canfield, and M. Lang, *Phys. Rev. B* **86**, 220511(R) (2012).
- [2] V. G. Kogan, L. N. Bulaevskii, P. Miranović, and L. Dobrosavljević-Grujić, *Phys. Rev. B* **51**, 15344 (1995).
- [3] V. G. Kogan, *Phys. Rev. B* **87**, 020503(R) (2013).
- [4] J. E. Ostenson, S. Bud'ko, M. Breitwisch, D. K. Finnemore, N. Ichikawa, and S. Uchida, *Phys. Rev. B* **56**, 2820 (1997).
- [5] H. Xiao, T. Hu, C. C. Almasan, T. A. Sayles and M. B. Maple, *Phys. Rev. B* **76**, 224510 (2007).
- [6] A. Cano, A. P. Levanyuk, and S. A. Minyukov, *Phys. Rev. B* **68**, 144515 (2003).
- [7] A. Cano, A. P. Levanyuk, and S. A. Minyukov, *Physica C* **404**, 226 (2004).
- [8] V. G. Kogan, *Phys. Rev. B* **88**, 144514 (2013).
- [9] S.-Z. Lin and V. G. Kogan, *Phys. Rev. B* **95**, 054511 (2017).
- [10] L. D. Landau and E. M. Lifshitz, *Electrodynamics of Continuous Media* (Elsevier, Amsterdam, 2006), Chap. 6.
- [11] L. D. Landau and E. M. Lifshitz, *Theory of Elasticity* (Pergamon, Oxford, 1986).
- [12] L. D. Landau and E. M. Lifshitz, *Fluid Mechanics* (Pergamon, Oxford, 1959).
- [13] L. D. Landau and E. M. Lifshitz, *Statistical Physics*, Part 1 (Elsevier Science, Amsterdam, 1980), Chap. 8.
- [14] L. N. Bulaevskii and E. M. Chudnovsky, *Phys. Rev. B* **72**, 094518 (2005).
- [15] L. Embon, Y. Anahory, Ž. L. Jelić, E. O. Lachman, Y. Myasoedov, M. E. Huber, G. P. Mikitik, A. V. Silhanek, M. V. Milosević, A. Gurevich, and E. Zeldov, *Nat. Commun.* **8**, 85 (2017).
- [16] A. E. Koshelev and V. M. Vinokur, *Phys. Rev. Lett.* **73**, 3580 (1994).
- [17] D. Li, A. M. Malkin, and B. Rosenstein, *Phys. Rev. B* **70**, 214529 (2004).
- [18] V. G. Kogan, *Phys. Rev. B* **97**, 094510 (2018).
- [19] B. Biehler, B.-U. Runge, P. Leiderer, and R. G. Mints, *Phys. Rev. B* **72**, 024532 (2005).